Observation of Reduced Cytotoxicity of Aggregated Amyloidogenic Peptides with Chaperone-like Molecules

Lei Liu,[†] Lan Zhang,[†] Lin Niu, Meng Xu, Xiaobo Mao, Yanlian Yang,[*] and Chen Wang[*]

National Center for Nanoscience and Technology, Beijing 100190, China. [†]These authors contributed equally to this work.

ABSTRACT The pathogenesis of many neurodegenerative diseases is associated with different types of aggregates of amyloidogenic peptides, including senile plaques, fibrils, protofibrils, and oligomers. It is therefore valuable to explore diversity of approaches toward reducing the cytotoxicity of amyloidogenic peptides by modulating aggregation behaviors. Herein we report an approach toward reducing the neuronal cytotoxicity of amyloidogenic peptides by accelerating the aggregation process, which is different from prevalent methods *via* inhibiting the aggregation of peptides. The pyridyl derivatives behave like chaperones to dramatically change the assembling characteristics of the peptides *via* strong hydrogen bond formation with C-termini of amyloid β (Aβ) peptides, which is revealed by using scanning probe microscopy. The light scattering experiments demonstrated the effect of the chaperone-like molecules on accelerating the aggregation process of Aβ peptides, accompanied by the reduced neuronal cytotoxicity of amyloidogenic peptides. These results would give rise to a complementary approach for modulating biological effects of the aggregates of amyloidogenic peptides.

KEYWORDS: amyloidogenic peptide · peptide aggregation · modulation · neuronal cytotoxicity · chaperone-like molecules

Protein misfolding[1,2] and abnormal assembling pathways are implicated in over 30 human disorders, including Alzheimer's disease (β-amyloid (Aβ) peptides), type II diabetes mellitus (human islet amyloid polypeptide), and transmissible spongiform encephalopathy (prion protein) *etc.*[3−11] The pathology of these human disorders is very likely correlated with self-assembly of amyloidogenic peptides into various forms of aggregates[12,13] such as oligomers, protofibrils, fibrils, and senile plaques. Recently, it has been reported that the concentration of soluble Aβ monomers and oligomers in the cerebral cortex is related to the degree of synaptic loss.[14−16] It is also reported that the oligomers of amyloidogenic peptides are more toxic to neurons in comparison with the fibril aggregates.[17] To reduce the cytotoxicity of these peptides (abnormal biological function), a variety of molecules have been designed to modulate the aggregation of amyloidogenic peptides. In general, two kinds of strategies, that is, inhibiting aggregation and disassembling aggregates of amyloidogenic peptides by designed small molecules and peptides, are applied to reduce the cytotoxicity of amyloidogenic peptides. Some organic dye molecules (Congo red, thioflavin T, and their derivatives) and the polyphenol compounds, such as tannic acid and curcumin, are excellent agents for inhibiting the fibrosis of amyloidogenic peptides.[18−23] Protein mimetics are also reported to behave as inhibitors of amyloidal peptide oligomerization.[24,25] β-Strands corresponding to 14−23 residues of Aβ were incorporated into green fluorescence protein with β-barrel structure to target and bind with Aβ monomers, leading to inhibition of the aggregation of Aβ peptides.[26] Alternatively, it is reported that apocyclen attached to Aβ recognition motifs, Aβ16−20 (KLVFF) could capture Cu(II) to become proteolytically active, and the complexes were capable of interfering with Aβ aggregation and degrading Aβ into fragments, as well as preventing H_2O_2 formation for reduced toxicity to neuronal cells.[27]

Recently, we have reported the interaction between chaperone-like molecules and the key fragment of amyloid β peptides Aβ33−42.[28] It was identified from light scattering results that pyridyl derivatives could interact with the peptide C-termini and appreciably accelerate the aggregation of Aβ33−42 peptides. It was also reported that polycations such as polylysine appended to KLVFF peptide by covalent bonding could increase the rate of fibril formation.[29] Copper and zinc ions have been shown to accelerate the aggregation of Aβ peptides.[30−32] Furthermore, the crowded environments are also capable of accelerating aggregation of amyloidogenic peptides.[33]

It is therefore plausible that the introduction of chaperone-like molecules could reduce the cytotoxicity of amyloidogenic peptides by accelerating the aggregation of peptides. In this work, we examine the cytotoxicity of the chaperone-like molecules on

* Address correspondence to wangch@nanoctr.cn, yangyl@nanoctr.cn.

Received for review May 15, 2011 and accepted June 18, 2011.

Published online June 19, 2011
10.1021/nn201773x

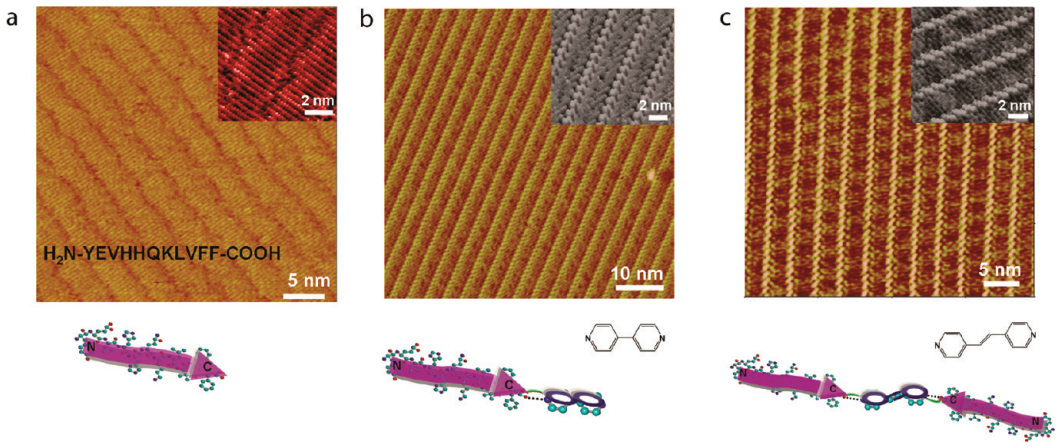

Figure 1. Assembly structure of amyloidogenic peptide and the modulated peptide assemblies by chaperone-like molecules. The two-dimensional STM images of (a) Aβ10−20, (b) Aβ10−20/4Bpy, and (c) Aβ10−20/DPE assemblies on HOPG surface. The inset images at the upper right corner correspond to high-resolution three-dimensional STM images. The amino acid sequence of Aβ10−20 is superimposed on the STM image in panel a. The proposed basic building block models for the peptides, peptide/molecule complex assemblies, are presented in the corresponding lower panels. The purple arrows represent the peptide strands and the blue circles are for the pyridyl moieties. The tentative molecular models for the peptide with extended strands are shown in a schematic way. The molecular structures of 4,4′-bipyridyl (4Bpy) and 1,2-di(4-pyridyl)-ethylene (DPE) are provided in panels b and c. The molecules 4Bpy and DPE bind to Aβ10−20 peptides *via* hydrogen bonds between carboxyl groups of Aβ10−20 and N atoms of pyridyl moieties. Tunneling conditions: (a) 792 mV and 405 pA, 500 mV and 299 pA (inset); (b) 770 mV and 464 pA, 770 mV and 464 pA (inset); (c) 709 mV and 495 pA, 709 mV and 495 pA (inset).

peptide Aβ10−20, which is a key fragment of amyloid peptide Aβ1−42. The pyridyl species are observed to coassemble with Aβ10−20 at molecular level *via* noncovalent interactions. Scanning probe microscopy is applied to study the assembly characteristics of the amyloidogenic peptides[28,34,35] due to its high structural resolution and adaptability to various environments.[28,34,36−39] The cell viability experiments revealed that the presence of the pyridyl species could appreciably reduce the cytotoxicity of the amyloidogenic peptides.

RESULTS AND DISCUSSION

Modulating Effect of Chaperone-like Molecules on Amyloidogenic Peptide Assembly at Molecular Level. After the solutions of peptide molecules or peptide with chaperone-like molecules are deposited onto the highly oriensted pyralytic graphite (HOPG) surface, the modulation effect at the molecular level was investigated with scanning tunneling microscopy (STM) after the solvent was completely evaporated. The observations of the peptide assembling characteristics reveal that Aβ10−20 peptides interact with each other to form lamella structures, as shown in Figure 1a. The Aβ10−20 peptides form β-sheet-like structures, and the lengths of the peptides are 3.45 nm, which is consistent with the expected value (the secondary structure and length statistic of Aβ10−20 peptide are shown in Figure S1a,b in the Supporting Information).

The molecules with pyridyl groups, 4,4′-bipyridyl (4Bpy) and 1,2-di(4-pyridyl)ethylene (DPE), were introduced to coassemble with Aβ10−20. The hybrid lamella structures of amyloidogenic peptides and molecules were formed as revealed in Figure 1b,c. The molecules 4Bpy and DPE bind to the amyloidogenic peptide Aβ10−20 *via* hydrogen bond between N atoms of the pyridyl moieties and the carboxyl groups of Aβ10−20 peptides.[28] The bright features in the linear arrays (Figure 1b,c) are the characteristics of 4Bpy and DPE molecules, and the stripe structures with reduced contrast represent the amyloidogenic peptides in STM images. There exist some structural differences between the two hybrid assemblies of Aβ10−20/4Bpy and Aβ10−20/DPE. One can identify from the STM images that one 4Bpy molecule is associated with one peptide, while one DPE is accompanied by two peptides. Such difference in assembling stoichiometry could be ascribed to the trans-conformation of the DPE molecules originated from the ethylene groups between two pyridyl groups (the proposed molecular models can be found in Figure S2a,b in Supporting Information). The antiparallel β-sheet secondary structures of amyloidogenic peptide Aβ10−20 with and without the two modulator molecules can be confirmed by the Fourier transform infrared (FTIR) spectra (Figure S3 in Supporting Information).

Modulating Effect on Amyloidogenic Peptide Aggregate Morphology. We further studied the modulating effects on the aggregation process that could be related to the molecular level assembling behaviors of the amyloidogenic peptides observed by STM. Atomic force microscopy (AFM) characterizations of the peptide assemblies on HOPG surfaces are conducted. The AFM image of the Aβ10−20 aggregates reveals typical fibril structures (Figure 2a). In the presence of the chaperone-like molecular species, short fibrils are

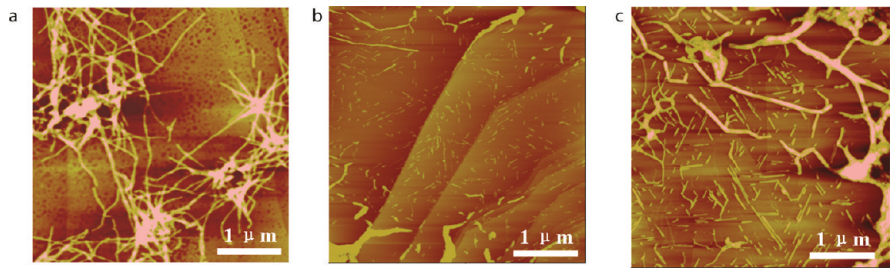

Figure 2. Aggregate morphologies of Aβ10−20 peptides and peptide/molecule complexes by AFM on HOPG surface. (a) Aβ10−20, mature fibrils; (b) Aβ10−20/4Bpy, and (c) Aβ10−20/DPE, short fibrils. The *z*-scales for all of the images are 20 nm. The chaperone-like molecules are capable of changing the aggregate morphology of amyloidogenic peptide Aβ10−20, forming short fibrils instead of mature fibrils.

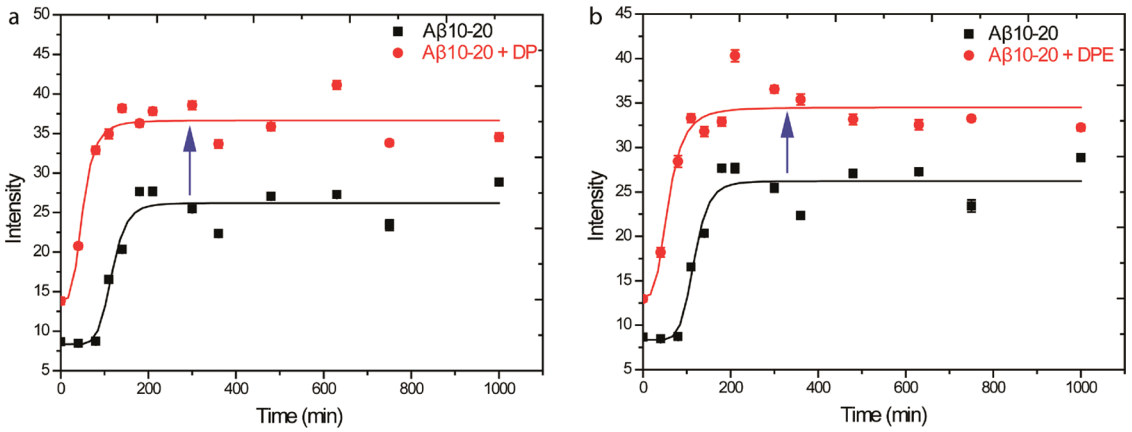

Figure 3. Modulation effects of (a) 4Bpy and (b) DPE on the aggregation process of Aβ10−20 in phosphate buffer as measured by light scattering. The legends are shown in panels a and b, respectively. The red and black solid lines are presented just for guiding the eyes. The blue arrows are indicative of accelerating effect of peptide aggregation in the presence of the chaperone-like molecules.

predominant in AFM images rather than the mature fibrils (Figure 2b,c). The discrepancies of aggregate morphologies of Aβ10−20 and Aβ10−20/modulators are due to the modulating effect on the assembly structures of Aβ10−20 peptides on a molecular level. The lengths of these short fibrils are 121 ± 22 nm (Aβ10−20/4Bpy) and 233 ± 67 nm (Aβ10−20/DPE), respectively (shown in Figure S4a,b), which are much more than the size of oligomers of amyloidogenic peptides with cytotoxicity (10−25 nm in lateral dimensions and 2−8 nm in height, as a reflection of diverse forms of peptide aggregates).[16,40,41]

Modulating Effect on Amyloidogenic Peptide Aggregation in Solution. To evaluate the impact of the molecular species on the aggregation of Aβ10−20 in aqueous solution, the aggregation was followed by turbidity measurements. It was clearly observed that the molecular species could accelerate the aggregation process in aqueous solution in comparison with neat Aβ10−20, as shown in Figure 3a,b. Control experiments showed the lower aggregation trends of 4Bpy and DPE (Figure S5) in comparison to Aβ10−20, thus the contribution of their aggregation can be neglected in the total light scattering intensities of the Aβ10−20/modulator systems. The mechanism of the accelerated aggregation could be attributed to the increased assembling kinetics by linking peptide stripes by the chaperone-like molecular species, as shown in Figure 1b,c.

It is reported that the cytotoxicity of amyloidogenic peptides could be reduced with either decreasing or increasing the dimension of peptide aggregates.[17,40,42] Therefore, it is feasible to reduce the cytotoxicity of the Aβ10−20 aggregates by introduction of the chaperone-like molecules. Furthermore, the molecular species are capable of regulating the kinetic aggregation behaviors of Aβ10−20 peptides, which would possibly reduce the occurrence probability and effective concentration of oligomers resulting in reduced cytotoxicity.

Modulating Effect on Reducing the Cytotoxicity of Amyloidogenic Peptides. The relevance of the observed variations in peptide aggregation behaviors with the cytotoxicity changes is also examined. Fresh solution of amyloidogenic peptides Aβ10−20 was found to have neuronal cytotoxicity by cell viability assays. The cell viability of SH-SY5Y cells treated with fresh Aβ10−20 solution is greatly decreased with increasing Aβ10−20 concentration from 10 to 200 μM (Figure 4a and Figure S6a in Supporting Information), which is consistent with the previous reports that the neuron injury is dependent on Aβ concentrations, rather than the Aβ plaque

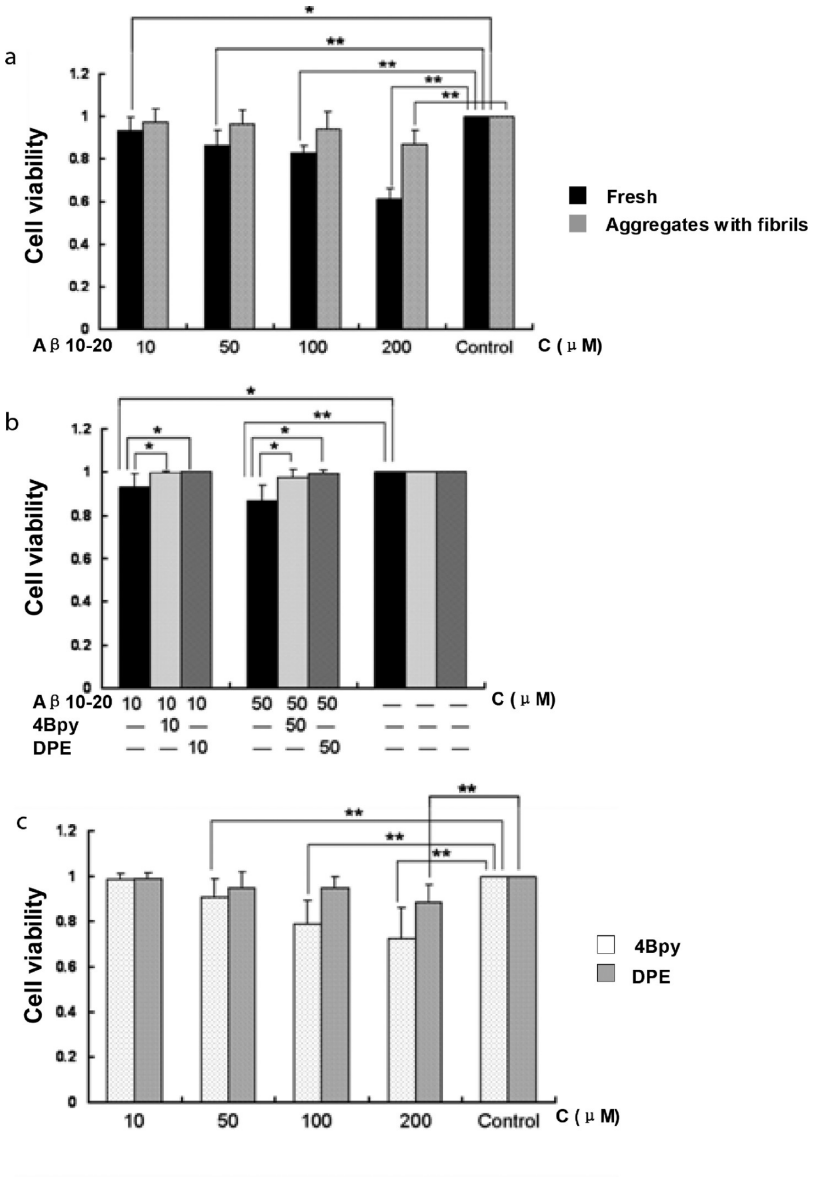

Figure 4. Cytotoxicity of amyloidogenic peptides and inhibition effect of the chaperone-like molecules on the cytotoxicity of the peptides. The cytotoxicity of (a) fresh Aβ10−20 solution and Aβ10−20 aggregates with fibrils incubated at 37 °C for 24 h. (b) Cell viability of Aβ10−20 in the absence and presence of 4Bpy and DPE measured by WST-8 toxicity assay. The chaperone-like molecules could reduce the cytotoxicity of amyloidogenic peptides to some extent. (c) Cell viability of 4Bpy and DPE with diverse concentrations. DPE molecule shows lower neuronal cytotoxicity in comparison with the 4Bpy molecule. Results are mean ± SD (n = 3). Statistical differences compared with the controls are given as *, $P < 0.05$ and **, $P < 0.01$.

burden.[14,43] After incubation of Aβ10−20 peptide *in vitro* at 37 °C for 24 h, the aggregation of Aβ10−20 will give rise to more fibrils or large aggregates than the samples incubated for 2 h (Figure 2a). The cell viability of the Aβ10−20 aggregates with fibrils (incubation for 24 h) in solution show greatly reduced neuronal cytotoxicity, which is opposite to the fresh solution of Aβ10−20 (Figure 4a). This result further confirmed the lower toxicity of the mature fibrils or large aggregates.

The above results reveal that the mature aggregates of amyloidogenic peptides are nearly noncytotoxic. These results illustrate the possibility of reducing cytotoxicity of amyloidogenic peptides by accelerating the aggregation of peptides with chaperone-like molecules into a state with mostly mature aggregates in a shorter time. When the molecules of 4Bpy and DPE were introduced to target the peptides *via* a hydrogen bond between the peptides and pyridyl molecules in fresh Aβ10−20 solution, the cytotoxicity of the peptides was greatly reduced at the Aβ10−20 concentration of 10 and 50 μM (Figure 4b). The cell viabilities of Aβ10−20/4Bpy and Aβ10−20/DPE shown in Figure S6b,c in Supporting Information reveal lower cytotoxicity than Aβ10−20, and DPE molecule demonstrates better potency than 4Bpy. The cytotoxicity discrepancy of two peptide/molecule complex systems could be possibly attributed to

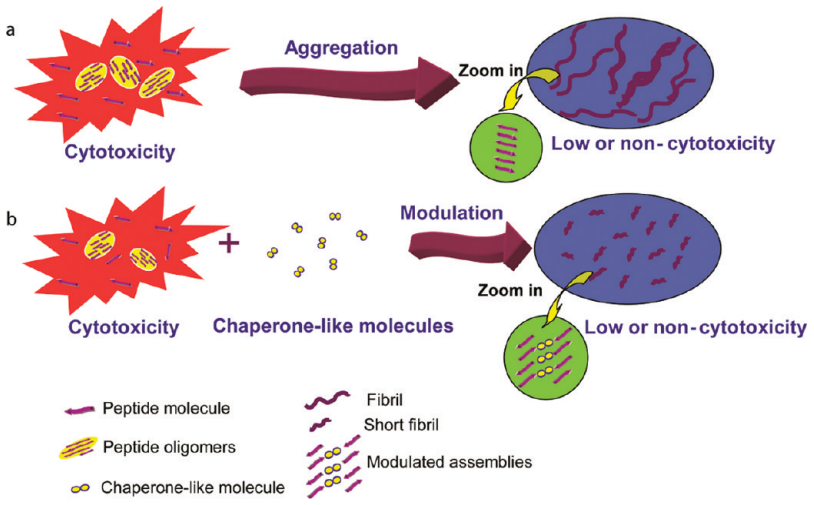

Figure 5. Schematic models for the modulation effect of chaperone-like molecules on aggregation behaviors and cytotoxicity of amyloidogenic peptides. (a) Cytotoxicity of the soluble monomeric and oligomeric amyloidogenic peptides and the lower or noncytotoxicity of the peptide aggregates with fibrils. (b) Accelerated aggregation process induced by the chaperone-like molecules leads to the faster formation of short fibrils of peptide/molecule complexes, which subsequently results in the reduced cytotoxicity of amyloidogenic peptides. The cytotoxicity is presented as a red explosive shape, and the blue ring represents lower or noncytotoxicity in both panels a and b. The fine structures of mature fibrils of amyloidogenic peptides, short fibrils of peptide/molecule complexes, are show in green rings. The detailed legends can be found at lower left corner.

different modulation effect of pyridyl molecules on the assembly structures of amyloidogenic peptides (Figure 2b,c). Another possible reason could be ascribed to the toxicity of the pyridyl molecules themselves to neuron cells (Figure 4c). The cell viabilities of DPE and 4Bpy suggest that the DPE molecule is preferential due to its lower cytotoxicity in our detection range.

It could be proposed that the mechanism of reducing the cytotoxicity *via* introduction of chaperone-like molecules is possibly correlated with the variation of the aggregation behaviors. In the previous reports, it is elucidated that cognitive impairment correlated better with cerebral Aβ concentrations than with amyloid plaque numbers[44] and correlated best with the soluble pool of cerebral Aβ, which contains soluble oligomers.[14,45,46] The concentrations of soluble Aβ monomers and oligomers in the cerebral cortex correlate with the degree of synaptic loss.[45] It has been hypothesized that these amyloidogenic peptide monomers and soluble oligomers might have interaction with the cell membrane and result in the cell dysfunction. The modulated peptide assembly with chaperone-like molecules could correlate with the faster aggregation from amyloidogenic peptide monomers and oligomers to large aggregates (Figure 2b,c and Figure 4b), which could be viewed as a similar effect on reducing amyloidogenic peptide cytotoxicity by incubation of Aβ10−20 peptide *in vitro* at 37 °C for 24 h (Figure 4a). The two approaches both block the interaction of the amyloidogenic peptide monomers and oligomers with cell membranes for reduction of toxic species to neurons.

It is clear that the molecular level studies of the aggregation behavior of amyloidogenic peptides could be relevant to the cytotoxicity of these peptides and also the inhibitory effects of the neuronal injury of these peptides. The schematic model is shown in Figure 5. The chaperone-like molecular species can target the termini, the main chains, or the side groups of peptides and modulate the assembly characteristics as well as the aggregation behaviors of peptides. The similar effect could be completed by incubating the peptides, which is a slow process (Figure 5a). 4Bpy and DPE were found to accelerate the Aβ assembly process and reduce the cytotoxicity appreciably. The results on the accelerated peptide aggregation process and the reduced toxic species could provide an alternative approach toward reducing the cytotoxicity of amyloidogenic peptides, complementary to the methods by inhibiting and disassembling the aggregation of peptides.[27,29,47]

CONCLUSIONS

In summary, we have demonstrated that noncovalent interactions between the peptide and organic molecule could be utilized to modulate the primary assembly structure of amyloidogenic peptides and subsequently the aggregation behaviors. The appreciably reduced cytotoxicity of amyloidogenic peptides was also observed in association with the accelerated aggregation process by the chaperone-like molecular species. These observations could be beneficial for obtaining insight into the interaction mechanism between protein, peptide, and drug molecules relating to amyloidosis

and also be of genuine interest for designing new functional molecules as therapeutic agents for amyloidosis based on a novel accelerating aggregation approach.

EXPERIMENTAL SECTION

Sample Preparation. Aβ10−20 was purchased from American Peptide Company, Inc. with a purity of 98%. It was dissolved in hexafluoroisopropanol (HFIP, Sigma) initially for an extended time, and the solution was transferred into a sterile microcentrifuge tube followed by evaporation of the HFIP solvent under vacuum. The obtained peptide deposits were dissolved in Milli-Q water. 4,4′-Bipyridyl and 1,2-di(4-pyridyl)ethylene were dissolved in ethanol, and then the peptide solution was mixed with the solutions of the pyridyl molecules to reach the final concentration *ca.* 0.1 mM. The mixed solutions were kept standstill for 2 h at 37 °C, then 5 μL of Aβ10−20 solutions or peptide/molecule complex solutions was dropped onto a freshly cleaved HOPG surface and then observed directly by STM after the solvent was evaporated. The samples for STM observations were also used for AFM investigations. The temperature of STM and AFM detection was about 30 °C in ambient conditions. The concentration of Aβ10−20 and the chaperone-like molecules for light scattering was 0.2 mM in phosphate buffer (5 mM sodium dihydrogen phosphate and sodium phosphate, and pH = 7.4) in the presence of 20 μL of DMSO. The samples for light scattering measurement were incubated at 37 °C.

STM Experiments. The STM experiments were carried out with a Nanoscope IIIa system (Veeco Metrology, USA) working at ambient conditions. Mechanically formed Pt/Ir (80%/20%) tips were used in the STM experiments. All STM images were obtained in constant current mode, and the tunneling conditions were shown in the corresponding figure captions.

AFM Investigations. Tapping mode AFM studies were performed on a Nanoscope IIID AFM instrument (Veeco Metrology, USA) under ambient conditions. Commercial silicon tips with a nominal spring constant of 40 N/m and resonant frequency of 300 kHz were used in all of the experiments.

Light Scattering Measurements. Light scattering was measured on a PerkinElmer LS55 fluorescence spectrophotometer at room temperature using 1 cm path length quartz cell. Both excitation and emission wavelengths were set to 400 nm with a spectrum bandwidth of 1 nm. The light scattering signal was quantified by averaging the emission intensity at 400 nm (slit width = 2.5 nm) over 15 s in an attenuation mode.

Cell Culture. SH-SY5Y human neuroblastoma cells (ECACC, UK) were cultured in DMEM (Gibco, Invitrogen, UK) containing 10 IU penicillin/mL (Gibco, Invitrogen, UK), 100 μg of streptomycin/mL (Gibco, Invitrogen, UK), and 10% fetal bovine serum (Hyclone, Invitrogen, UK). The cells were routinely subcultured once every 3 days at a dilution of 1:2 and grown at 37 °C in a 95% air/5% CO_2 humidified incubator (Sanyo, UK) in 75 cm^3 tissue culture-treated flasks (Nalge Nunc International, Naperville, IL, USA).

Cell Viability Assay. SH-SY5Y cells were plated at a concentration of 10 000 cells/well (100 μL/well) in 96-well plates (Greiner Bio-One Inc., Longwood, FL, USA) in full medium and incubated overnight at 37 °C. Then SH-SY5Y neurons were treated with or without various concentrations of fresh Aβ10−20 in the presence or absence of chaperone-like molecules for 48 h. The Aβ10−20 aggregates with fibrils were incubated at 37 °C for 24 h before being applied to the cell culture medium for SH-SY5Y cells. The WST-8 cell viability assay was performed by using Cell Counting Kit-8 (Dojindo Laboratories, Kumanoto, Japan), according to the supplier recommendations. Cell viability was expressed as the percentage of viable cell relative to untreated cells using the absorbance at 450 nm.

Statistical Analyses. Experiments are means of triplicates. Data are expressed as mean ± standard deviation (SD). Statistical analyses were performed with SPSS (SPSS, Chicago) by using a paired *t*-test. Differences were considered statistically significant when $P < 0.05$.

Acknowledgment. The authors thank Prof. X.J. Liang at the National Center for Nanoscience and Technology for great help in providing cell culture facilities. The authors also wish to thank Prof. Y.M. Li from Tsinghua University for very helpful discussions. This work was supported by the National Basic Research Program of China (2009CB930100) and Chinese Academy of Sciences (KJCX2-YW-M15). Financial support from National Natural Science Foundation of China (20911130229) and CAS Key Laboratory for Biological Effects of Nanomaterials & Nanosafety is also gratefully acknowledged.

Supporting Information Available: Experimental details for FTIR; the secondary structures of Aβ10−20, Aβ10−20/4Bpy, and Aβ10−20/DPE; the structural models for Aβ10−20/4Bpy and Aβ10−20/DPE complexes; the statistical histograms of the length distributions of the Aβ10−20/4Bpy and Aβ10−20/DPE aggregates; the aggregation behaviors of 4Bpy and DPE by light scattering; cell viabilities of Aβ10−20, Aβ10−20/4Bpy, and Aβ10−20/DPE. This material is available free of charge *via* the Internet at http://pubs.acs.org.

REFERENCES AND NOTES

1. Chiti, F.; Dobson, C. M. Protein Misfolding, Functional Amyloid, and Human Disease. *Annu. Rev. Biochem.* **2006**, *75*, 333–366.
2. Dobson, C. M. Protein Folding and Misfolding. *Nature* **2003**, *426*, 884–890.
3. Goedert, M.; Spillantini, M. G. A Century of Alzheimer's Disease. *Science* **2006**, *314*, 777–781.
4. Roberson, E. D.; Mucke, L. 100 Years and Counting: Prospects for Defeating Alzheimer's Disease. *Science* **2006**, *314*, 781–784.
5. Brody, D. L.; Magnoni, S.; Schwetye, K. E.; Spinner, M. L.; Esparza, T. J.; Stocchetti, N.; Zipfel, G. J.; Holtzman, D. M. Amyloid-Beta Dynamics Correlate with Neurological Status in the Injured Human Brain. *Science* **2008**, *321*, 1221–1224.
6. Forloni, G.; Angeretti, N.; Chiesa, R.; Monzani, E.; Salmona, M.; Bugiani, O.; Tagliavini, F. Neurotoxicity of a Prion Protein-Fragment. *Nature* **1993**, *362*, 543–546.
7. Kahn, S. E.; Andrikopoulos, S.; Verchere, C. B. Islet Amyloid: A Long-Recognized but Underappreciated Pathological Feature of Type 2 Diabetes. *Diabetes* **1999**, *48*, 241–253.
8. Westermark, P.; Wilander, E. Influence of Amyloid Deposits on Islet Volume in Maturity Onset Diabetes-Mellitus. *Diabetologia* **1978**, *15*, 417–421.
9. Young, A. A.; Gedulin, B.; Vine, W.; Percy, A.; Rink, T. J. Gastric-Emptying Is Accelerated in Diabetic Bb Rats and Is Slowed by Subcutaneous Injections of Amylin. *Diabetologia* **1995**, *38*, 642–648.
10. Maloy, A. L.; Longnecker, D. S.; Greenberg, E. R. The Relation of Islet Amyloid to the Clinical Type of Diabetes. *Hum. Pathol.* **1981**, *12*, 917–922.
11. Lorenzo, A.; Razzaboni, B.; Weir, G. C.; Yankner, B. A. Pancreatic-Islet Cell Toxicity of Amylin Associated with Type-2 Diabetes-Mellitus. *Nature* **1994**, *368*, 756–760.
12. Kelly, J. W. Towards an Understanding of Amyloidogenesis. *Nat. Struct. Mol. Biol.* **2002**, *9*, 323–325.
13. Dobson, C. M. Protein Misfolding, Evolution and Disease. *Trends Biochem. Sci.* **1999**, *24*, 329–332.
14. Selkoe, D. J. Folding Proteins in Fatal Ways. *Nature* **2003**, *426*, 900–904.
15. Klein, W. L. A-Beta Toxicity in Alzheimer's Disease: Globular Oligomers (ADDLs) as New Vaccine and Drug Targets. *Neurochem. Int.* **2002**, *41*, 345–352.
16. Lambert, M. P.; Barlow, A. K.; Chromy, B. A.; Edwards, C.; Freed, R.; Liosatos, M.; Morgan, T. E.; Rozovsky, I.; Trommer, B.; Viola, K. L.; *et al.* Diffusible, Nonfibrillar Ligands Derived

from A Beta(1−42) Are Potent Central Nervous System Neurotoxins. *Proc. Natl. Acad. Sci. U.S.A.* **1998**, *95*, 6448–6453.
17. Bucciantini, M.; Giannoni, E.; Chiti, F.; Baroni, F.; Formigli, L.; Zurdo, J. S.; Taddei, N.; Ramponi, G.; Dobson, C. M.; Stefani, M. Inherent Toxicity of Aggregates Implies a Common Mechanism for Protein Misfolding Diseases. *Nature* **2002**, *416*, 507–511.
18. Frid, P.; Anisimov, S. V.; Popovic, N. Congo Red and Protein Aggregation in Neurodegenerative Diseases. *Brain Res. Rev.* **2007**, *53*, 135–160.
19. Klunk, W. E.; Debnath, M. L.; Pettegrew, J. W. Development of Small-Molecule Probes for the Beta-Amyloid Protein of Alzheimers-Disease. *Neurobiol. Aging* **1994**, *15*, 691–698.
20. Gestwicki, J. E.; Crabtree, G. R.; Graef, I. A. Harnessing Chaperones To Generate Small-Molecule Inhibitors of Amyloid Beta Aggregation. *Science* **2004**, *306*, 865–869.
21. Ono, K.; Naiki, H.; Yamada, M. The Development of Preventives and Therapeutics for Alzheimer's Disease That Inhibit the Formation of Beta-Amyloid Fibrils (fA beta), as Well as Destabilize Preformed fA Beta. *Curr. Pharm. Des.* **2006**, *12*, 4357–4375.
22. Hamaguchi, T.; Ono, K.; Murase, A.; Yamada, M. Phenolic Compounds Prevent Alzheimer's Pathology through Different Effects on the Amyloid-Beta Aggregation Pathway. *Am. J. Pathol.* **2009**, *175*, 2557–2565.
23. Yang, F. S.; Lim, G. P.; Begum, A. N.; Ubeda, O. J.; Simmons, M. R.; Ambegaokar, S. S.; Chen, P. P.; Kayed, R.; Glabe, C. G.; Frautschy, S. A.; *et al.* Curcumin Inhibits Formation of Amyloid Beta Oligomers and Fibrils, Binds Plaques, and Reduces Amyloid *In Vivo*. *J. Biol. Chem.* **2005**, *280*, 5892–5901.
24. Gibson, T. J.; Murphy, R. M. Design of Peptidyl Compounds That Affect Beta-Amyloid Aggregation: Importance of Surface Tension and Contex. *Biochemistry* **2005**, *44*, 8898–8907.
25. Pallitto, M. M.; Ghanta, J.; Heinzelman, P.; Kiessling, L. L.; Murphy, R. M. Recognition Sequence Design for Peptide Modulators of Beta-Amyloid Aggregation and Toxicity. *Biochemistry* **1999**, *38*, 3570–3578.
26. Takahashi, T.; Ohta, K.; Mihara, H. Embedding the Amyloid Beta-Peptide Sequence in Green Fluorescent Protein Inhibits A Beta Oligomerization. *ChemBioChem* **2007**, *8*, 985–988.
27. Wu, W. H.; Lei, P.; Liu, Q.; Hu, J.; Gunn, A. P.; Chen, M. S.; Rui, Y. F.; Su, X. Y.; Xie, Z. P.; Zhao, Y. F.; *et al.* Sequestration of Copper from Beta-Amyloid Promotes Selective Lysis by Cyclen-Hybrid Cleavage Agents. *J. Biol. Chem.* **2008**, *283*, 31657–31664.
28. Liu, L.; Zhang, L.; Mao, X. B.; Niu, L.; Yang, Y. L.; Wang, C. Chaperone-Mediated Single Molecular Approach toward Modulating Aβ Peptide Aggregation. *Nano Lett.* **2009**, *9*, 4066–4072.
29. Stains, C. I.; Mondal, K.; Ghosh, I. Molecules That Target Beta-Amyloid. *ChemMedChem* **2007**, *2*, 1675–1692.
30. Bush, A. I.; Pettingell, W. H.; Multhaup, G.; Paradis, M. D.; Vonsattel, J. P.; Gusella, J. F.; Beyreuther, K.; Masters, C. L.; Tanzi, R. E. Rapid Induction of Alzheimer A-Beta Amyloid Formation by Zinc. *Science* **1994**, *265*, 1464–1467.
31. Lovell, M. A.; Robertson, J. D.; Teesdale, W. J.; Campbell, J. L.; Markesbery, W. R. Copper, Iron and Zinc in Alzheimer's Disease Senile Plaques. *J. Neurol. Sci.* **1998**, *158*, 47–52.
32. Cherny, R. A.; Legg, J. T.; McLean, C. A.; Fairlie, D. P.; Huang, X. D.; Atwood, C. S.; Beyreuther, K.; Tanzi, R. E.; Masters, C. L.; Bush, A. I. Aqueous Dissolution of Alzheimer's Disease A Beta Amyloid Deposits by Biometal Depletion. *J. Biol. Chem.* **1999**, *274*, 23223–23228.
33. White, D. A.; Buell, A. K.; Knowles, T. P. J.; Welland, M. E.; Dobson, C. M. Protein Aggregation in Crowded Environments. *J. Am. Chem. Soc.* **2010**, *132*, 5170–5175.
34. Ma, X. J.; Liu, L.; Mao, X. B.; Niu, L.; Deng, K.; Wu, W. H.; Li, Y. M.; Yang, Y. L.; Wang, C. Amyloid Beta (1−42) Folding Multiplicity and Single-Molecule Binding Behavior Studied with STM. *J. Mol. Biol.* **2009**, *388*, 894–901.
35. Mao, X. B.; Ma, X. J.; Liu, L.; Niu, L.; Yang, Y. L.; Wang, C. Structural Characteristics of the Beta-Sheet-like Human and Rat Islet Amyloid Polypeptides As Determined by Scanning Tunneling Microscopy. *J. Struct. Biol.* **2009**, *167*, 209–215.
36. Yang, Y. L.; Wang, C. Hierarchical Construction of Self-Assembled Low-Dimensional Molecular Architectures Observed by Using Scanning Tunneling Microscopy. *Chem. Soc. Rev.* **2009**, *38*, 2576–2589.
37. Kudernac, T.; Lei, S. B.; Elemans, J.; De Feyter, S. Two-Dimensional Supramolecular Self-Assembly: Nanoporous Networks on Surfaces. *Chem. Soc. Rev.* **2009**, *38*, 402–421.
38. Lingenfelder, M.; Tomba, G.; Costantini, G.; Ciacchi, L. C.; De Vita, A.; Kern, K. Tracking the Chiral Recognition of Adsorbed Dipeptides at the Single-Molecule Level. *Angew. Chem., Int. Ed.* **2007**, *46*, 4492–4495.
39. Wang, Y.; Lingenfelder, M.; Classen, T.; Costantini, G.; Kern, K. Ordering of Dipeptide Chains on Cu Surfaces through 2D Cocrystallization. *J. Am. Chem. Soc.* **2007**, *129*, 15742–15743.
40. Mahiuddin, A.; Judianne, D.; Darryl, A.; Takeshi, S.; Shivani, A.; Saburo, A.; James, I. E.; William, E. V. N.; Smith, S. O. Structural Conversion of Neurotoxic Amyloid-β_{1-42} Oligomers to Fibrils. *Nat. Struct. Mol. Biol.* **2010**, *17*, 561–568.
41. Mastrangelo, I. A.; Ahmed, M.; Sato, T.; Liu, W.; Wang, C. P.; Hough, P.; Smith, S. O. High-Resolution Atomic Force Microscopy of Soluble Aβ42 Oligomers. *J. Mol. Biol.* **2006**, *358*, 106–119.
42. Quist, A.; Doudevski, L.; Lin, H.; Azimova, R.; Ng, D.; Frangione, B.; Kagan, B.; Ghiso, J.; Lal, R. Amyloid Ion Channels: A Common Structural Link for Protein-Misfolding Disease. *Proc. Natl. Acad. Sci. U.S.A.* **2005**, *102*, 10427–10432.
43. Mucke, L.; Masliah, E.; Yu, G. Q.; Mallory, M.; Rockenstein, E. M.; Tatsuno, G.; Hu, K.; Kholodenko, D.; Johnson-Wood, K.; McConlogue, L. High-Level Neuronal Expression of A Beta(1−42) in Wild-Type Human Amyloid Protein Precursor Transgenic Mice: Synaptotoxicity without Plaque Formation. *J. Neurosci.* **2000**, *20*, 4050–4058.
44. Naslund, J.; Haroutunian, V.; Mohs, R.; Davis, K. L.; Davies, P.; Greengard, P.; Buxbaum, J. D. Correlation between Elevated Levels of Amyloid Beta-Peptide in the Brain and Cognitive Decline. *JAMA* **2000**, *283*, 1571–1577.
45. Kuo, Y. M.; Emmerling, M. R.; VigoPelfrey, C.; Kasunic, T. C.; Kirkpatrick, J. B.; Murdoch, G. H.; Ball, M. J.; Roher, A. E. Water-Soluble A Beta (N-40, N-42) Oligomers in Normal and Alzheimer Disease Brains. *J. Biol. Chem.* **1996**, *271*, 4077–4081.
46. Lue, L. F.; Kuo, Y. M.; Roher, A. E.; Brachova, L.; Shen, Y.; Sue, L.; Beach, T.; Kurth, J. H.; Rydel, R. E.; Rogers, J. Soluble Amyloid Beta Peptide Concentration as a Predictor of Synaptic Change in Alzheimer's Disease. *Am. J. Pathol.* **1999**, *155*, 853–862.
47. Takahashi, T.; Mihara, H. Peptide and Protein Mimetics Inhibiting Amyloid Beta-Peptide Aggregation. *Acc. Chem. Res.* **2008**, *41*, 1309–1318.